Original Article

www.jmss.mui.ac.ir

Impulse Noise Cancellation of Medical Images Using Wavelet Networks and Median Filters

Amir Reza Sadri, Maryam Zekri[1,2], Saeid Sadri[1,2], Niloofar Gheissari

Department of Electrical and Computer Engineering, [1]Department of Electrical and Engineering, Isfahan University of Technology, [2]Medical Image and Signal Processing Research Center, Isfahan University of Medical Sciences, Isfahan, Iran

Submission: 05-01-2012 Accepted: 17-01-2012

ABSTRACT

This paper presents a new two-stage approach to impulse noise removal for medical images based on wavelet network (WN). The first step is noise detection, in which the so-called gray-level difference and average background difference are considered as the inputs of a WN. Wavelet Network is used as a preprocessing for the second stage. The second step is removing impulse noise with a median filter. The wavelet network presented here is a fixed one without learning. Experimental results show that our method acts on impulse noise effectively, and at the same time preserves chromaticity and image details very well.

Key words: *Average background difference, gray-level difference, impulse noise, wavelet network*

INTRODUCTION

Image enhancement of medical images has attracted attention of researchers nowadays. Medical imaging is the technique and process used to create images of the human body for clinical purposes or medical science. It is widely acclaimed as a hallmark of modern medicine. Diagnostic imaging is an umbrella term for a wide variety of scans, examinations and images that are used in the field of medicine such as X-ray, computed tomography (CT), magnetic resonance imaging (MRI), ultrasound (US) and dermoscopy images (DI).[1] There is no doubt that medical imaging solution technology plays a vital role in the diagnosis and treatment of patients suffering from serious illness. Unfortunately, medical images encounter a various number of noises such as Gaussian, Poisson, Rician and impulse noise (salt and pepper noise).[2] This study focuses on impulse noise as medical images are mainly prone to this type of noise.

Impulse noise is frequently encountered in acquisition, transmission, storage and processing of images. The presence of impulse noise in an image may be either relatively high or low. Thus, it could severely degrade the image quality and cause some loss of image information details. Filtering a digital image to remove noise while keeping the image details is an essential part of this task. Various filtering techniques have been proposed for removing impulse noise in the literature: mean and median filters,[3] generalized trimmed mean filter,[4] adaptive median filter,[5] generalized morphological filters,[6] homomorphic and adaptive order statistics filters,[7] wavelet filters,[8,9] curvelet filters,[10] fuzzy Algorithms,[11,12] etc. It is well known that linear filters could produce serious image blurring. As a result, nonlinear filters have been widely exploited due to their improved filtering performance. Vector median filter (VMF),[13] provides efficient impulse noise attenuation. However, it treats all pixels of a color image in the same way and also modifies pixels that are not corrupted by noise. This is a serious issue in medical image analysis because loss of image details results in inaccurate image analysis which may prove fatal to the life of a person. Hence, many methods have been proposed for noise removal from medical images. While some of these methods use complicated formulations, others require deep knowledge about image noise factors. Hence, a simple noise reduction method that removes noise well and preserves at the same time image details without relying on image noise factors is desirable.[12] To avoid the damage of uncorrupted pixels, two-step filtering methods (e.g.[14,15]) can be used. The idea is based on impulse noise detection and noise removal. In,[14] a type of these two-step methods based on neural network and fuzzy decision is presented. In the first stage, an adaptive two-level feed forward neural network (NN) with a back propagation training algorithm was applied to remove the impulse noise from gray-scale images. Three inputs (gray-level difference (GD), average background difference (ABD)

Address for correspondence:
Amir Reza Sadri, Department of Electrical and Computer Engineering, Isfahan University of Technology, Isfahan, Iran.
E-mail: ar_sadry@yahoo.com

and accumulation complexity difference (ACD)) are defined which are the inputs of neural network.

wavelet network (WN) is a network based on wavelet transforms[16,17] in which discrete wavelet function is used as node activation function. In fact, the wavelet space is used as characteristic space of the pattern recognition task. Furthermore, WN combines the advantages of time frequency localization wavelet transform with the Classifying power of neural network. This increases accuracy and robustness.[18] The main advantage of wavelet networks over similar architectures such as multi-layer perceptrons (MLP) and networks of radial basis functions (RBF) is the possibility of optimizing the wavelet network structure by means of efficient deterministic construction algorithms. However, owing to the localized nature of the wavelet basis functions, wavelet networks may not be well suited to deal with high-dimensional data. Since the efficient procedure of selecting wavelets used in the OLS method is not very sensitive to the input dimension.[18] The OLS algorithm transforms the set of regressor vectors into a set of orthogonal basis vectors, so that it is possible to calculate the contribution degree of each basis vector to the output energy.[19]

In this paper, a new impulse noise removal technique based on wavelet network is proposed to restore digital images corrupted by impulse noise. First, wavelet network is employed to detect the noisy-pixels and distinguish it from noise free pixels. The WN inputs are two parameters GD and ABD that have been calculated before. Second, the median filter improves the noisy pixels. A series of experimental results show that the proposed method unlike conventional filters is capable of effectively eliminating the impulse noise while preserving more fine details. The wavelet network proposed here is a fixed grid wavelet network in which translation and dilation parameters are already determined and only the weights of network are optimized by training the network. In general, gradient type algorithms are not necessary to train such a network. Here orthogonal least square (OLS) algorithm is used to determine the network size and the values of parameters. In comparison with back propagation (BP), OLS is a much faster approach.

In,[14] for first step of noise removal algorithm, a neural network with tree inputs (GD, ABD and ACD) with 6000 pixel in training step, for only gray-scale images, is used. But in our study, a WN with two inputs (GD and ABD) with 1000 pixel for both gray-scale and color medical images without learning step and with less neurons in a hidden layer is presented.

In some recent papers such as,[20-23] impulse noise reduction has been investigated, but our approach which is algorithm based on fixed grid WN is not compared with these methods in this paper.

This paper is organized as follows. The basic concepts of two types of wavelet network are introduced in wavelet network. In this section, the WN structure with two algorithms necessary for formation of the network and determination of its parameters are presented. In impulse noise removal, impulse noise model and an algorithm for detecting and cancelling it based on wavelet network and median filter is introduced. The simulation results of the proposed method in comparison with other approaches are illustrated in experimental result. Finally, in conclusion, the summary and conclusion of the findings of the study are provided.

WAVELET NETWORK

A wavelet network is a nonlinear regression structure that implements input–output mappings as the superposition of dilated and translated versions of a mother wavelet function, which is localized both in the space and frequency domains.[24] Existing WNs can be classified into the following two types.[25]

- *Adaptive WNs*, where wavelets as activation functions stem from the continuous wavelet transform and the unknown parameters of the networks include the weighting coefficients (the outer parameters of the network) and the dilation and translation factors of the wavelets (the inner parameters of the network). These parameters can be viewed as coefficients varying continuously as in conventional neural networks and can be learned by gradient type algorithms.
- *Fixed grid WNs*, where the activation functions stem from the discrete wavelet transforms and unlike in adaptive neural networks, the unknown inner parameters of the networks vary on some fixed discrete lattices. In such a WN, the positions and dilations of the wavelets are fixed (predetermined) and only the weights have to be optimized by training the network. In general, gradient type algorithms are not necessary to train such a network. An alternative solution for training this type of network is to convert the networks into a linear-in-the-parameter problem, which can then be solved using least squares type algorithms.

According to,[17] the concept of adaptive WNs is an approximation route which combined the mathematical rigor of wavelets with the adaptive learning scheme of conventional neural networks into a single unit. Clearly, to train an adaptive WN, the gradients with respect to all the unknown parameters have to be expressed explicitly. The calculation of gradients may be heavy and complicated in some cases especially for high-dimensional models. In addition, most gradient type algorithms are sensitive to initial conditions, that is, the initialization of wavelet networks is extremely important to obtain a fast convergence for a given algorithm.[19] Another problem that needs to be considered for training an adaptive WN is how

to determine the initial number of wavelets associated with the network. These drawbacks often limit the application of adaptive WNs to low dimensions for dynamical identification problems. Unlike adaptive WNs, in a fixed grid WN, the number of wavelets as well as the scale and translation parameters can be determined in advance. The only unknown parameters are the weighting coefficients, that is, the outer parameters, of the network. The WN is now a linear-in-the-parameters regression, which can then be solved using least squares techniques.

Structure of Wavelet Network

The output signal of a wavelet network with one output y, d inputs $\{x_1,x_2,...,x_d\}$ and q nodes in the hidden layer is given in Eq.(1)

$$y = \sum_{i=1}^{q} \omega_i \psi_{a_i,t_i}(\boldsymbol{x}) \tag{1}$$

where $x=\{x_1,x_2,...,x_d\}^T$ is the vector of inputs, $\omega_i, i=1,2,...,q$ are weight coefficients between hidden and output layers, an ψ_{a_i,t_i} are dilated and translated versions of a mother wavelet function $\psi:\mathbb{R}^d\rightarrow\mathbb{R}$:

$$\psi_{a_i,t_i}(\boldsymbol{x}) = a_i^{-d/2}\psi\left(\frac{\boldsymbol{x}-\boldsymbol{t}_i}{a_i}\right) \tag{2}$$

Function ψ, termed as the mother wavelet, is required to have zero mean and also to be localized both in the space and frequency domains.[18] A number of methods are available to construct multidimensional mother wavelets (i.e., with $d>1$) from one-dimensional functions $\psi:\mathbb{R}\rightarrow\mathbb{R}$ with fast decay in space and frequency.[17] In the present study, the radial wavelets are used to implement WNs. For example the d dimensional Mexican hat wavelet can be expressed as

$$\psi(\boldsymbol{x}) = \eta\|\boldsymbol{x}\| = (d-\|\boldsymbol{x}\|^2)\exp(-\|\boldsymbol{x}\|^2/2)\,. \tag{3}$$

In Eq. (2), pairs (a_i,t_i) are taken from a grid Λ given by

$$\Lambda = \{(\alpha^{-m}, \boldsymbol{n}\beta\alpha^{-m}) : m\in\mathbb{Z}, \boldsymbol{n}\in\mathbb{Z}^d\}\,, \tag{4}$$

where the scalar parameters α and β define the step sizes of dilation and translation discretization, respectively. Typical choices for α, β are $\alpha=2$ and $\beta=1$ which are adopted throughout this work. So $(a_i,t_i)=(2^{-mi},n_i\,2^{-mi})$ and then the output of WN is given by

$$y = \sum_{i=1}^{q}\omega_i\psi_{m_i,\boldsymbol{n}_i}(\boldsymbol{x}) = \sum_{i=1}^{q}\omega_i\,2^{-m_i d/2}\psi_{m_i,\boldsymbol{n}_i}(2^{m_i}\boldsymbol{x}-\boldsymbol{n}_i)\,. \tag{5}$$

According to above definitions, any function $f\in L^2(\mathbb{R}^d)$ (finite-energy and continuous or discontinuous) can be approximated by an arbitrary precision using the wavelet network given in Figure 1 with Eq. (5).

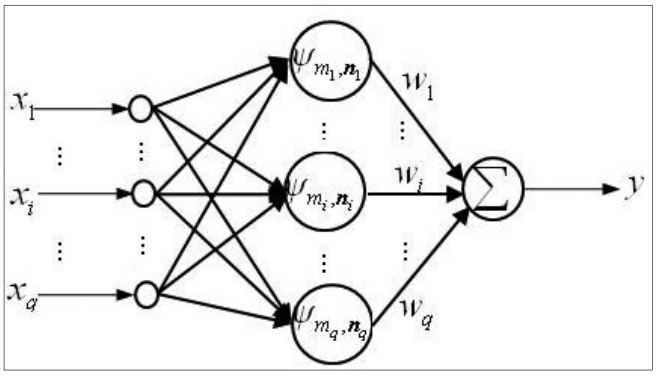

Figure 1: Wavelet network structure

Building a Wavelet Network

A major advantage of wavelet networks over other neural architectures is the availability of efficient construction algorithms for defining the network structure, that is, for choosing convenient values for (m,n) in (4). After the structure has been determined, the weights ω_i in (5) can be obtained through linear estimation techniques. In this work, a constructive method similar to that introduced in[18] and[24] is employed to build a wavelet network. It can be described as follows:

Algorithm1. *(Model construction)* Suppose that modeling samples are available in the form of input-output pairs, $(x[k], y[k])$, $k = 1,2,\ldots, M$, where $(x[k])_{d\times 1}$ is a column vector. Then;

1. Normalize the input data to fit within the effective support H of the mother wavelet employed. For radial wavelets, H is a hypersphere in $\mathbb{R}^d$ with radius R. For computational simplicity, H is approximated as a hypercube inscribed in the hypersphere with edges parallel to the coordinate axis.
2. Choose m_{min} and m_{max} the minimum and maximum scale levels to be employed.
3. For each sample $x[k]$ in the modeling set, find I_k the index set of wavelets whose effective supports contain $x[k]$:

$$I_k = \{(m,\boldsymbol{n}) : \boldsymbol{x}[k]\in H_{m,\boldsymbol{n}}; m_{min}\le m\le m_{max}\}\,, \tag{6}$$

   where, $H_{m,n}$ is a hypercube centered at $\boldsymbol{n}2^m$ with edges $2^m R\sqrt{2}$.
4. Determine the pairs $(m, \boldsymbol{n})$ which appear in at least two sets I_{k1} and I_{k2}, $k_1\neq k_2$. These are the wavelets whose effective supports include at least two samples. This step is different from the algorithm described in,[18] which allows for wavelets with effective supports containing only one sample. Such wavelets are not included here because they would introduce oscillations between neighbor modeling points, which might compromise the generalization ability of the model.
5. Let L be the number of wavelets obtained in

the previous step. For notational simplicity replace the double index (*m, n*) by a single index $i=1,...,L$. Apply the L wavelets to the M modeling samples and gather the results in a matrix form as follows:

$$W_{M\times L}=\begin{bmatrix}\psi_1(\boldsymbol{x}[1]) & \psi_2(\boldsymbol{x}[1]) & \cdots & \psi_L(\boldsymbol{x}[1])\\ \psi_1(\boldsymbol{x}[2]) & \psi_2(\boldsymbol{x}[2]) & \cdots & \psi_L(\boldsymbol{x}[2])\\ \vdots & \vdots & \cdots & \vdots\\ \psi_1(\boldsymbol{x}[M]) & \psi_2(\boldsymbol{x}[M]) & \cdots & \psi_L(\boldsymbol{x}[M])\end{bmatrix} \quad (7)$$

After these stages, the WN can then be converted into form

$$y=\sum_{i=1}^{L}\omega_i\psi_i(\boldsymbol{x})=W.\theta \quad (8)$$

Where, $\theta_{L\times 1}=\begin{bmatrix}\omega_1 & \cdots & \omega_L\end{bmatrix}^T$.

It is often the case that Steps 1 to 4 of the construction process result in a large number of wavelets. In order to avoid overfitting problems that result from an overparameterization of the model, it is then important to select a reduced subset of wavelets. A fast and efficient model structure determination approach has been implemented using the OLS algorithm. This approach has been extensively studied and widely applied in nonlinear system identification.[26] According to OLS algorithm, assume that we want to select the best subset of W while the size of this subset is known and denoted as s. At first, the most significant wavelets in W is selected. Next, all other (not selected) wavelets are made orthogonal to the selected one. In the second step of the algorithm the most significant of remaining wavelets is again selected and all non-selected wavelets are made orthogonal with respect to the selected one, and so on. Since all remaining wavelets are made orthogonal to all selected ones in each step of the algorithm, the improvement of each selectable wavelet is isolated. The iterative procedure is described in.[18]

After employ OLS algorithm the WN is constructed as

$$y=\sum_{i=1}^{s}\omega_i\psi_i(\boldsymbol{x}), \quad (9)$$

where s is the number of neuron in hidden layer and ω_i is weight of neurons.

IMPULSE NOISE REMOVAL

Impulse Noise Model

Impulse noise is when the pixels are randomly misfired and replaced by other values in an image. The image model containing impulse noise can be described as follows

$$X_{i,j}=\begin{cases}N_{i,j} & \text{with probability } p\\ S_{i,j} & \text{with probability } 1-p\end{cases} \quad (10)$$

where S_{ij} denotes the noiseless image pixel and N_{ij} denotes the noisy pixel replaced instead of original pixel. Parameter p shows the rate by which the image is corrupted by impulse noise. In a variety of impulse noise models for images, fixed- and random valued impulse noises are mostly discussed. Fixed-valued impulse noise, known as the salt-and pepper noise, is made up of corrupted pixels whose values are replaced with values equal to the maximum or minimum (255 or 0) of the allowable range.[14] This paper deals with the fixed impulse noise.

Noise Detection Algorithm

Since the residual noise will strongly affect human perception, precise noise detection is an essential step for the noise removal. The decision-based algorithms for noise detection can be divided into three types. The first type is to detect whether the pixel is contaminated by noise according to the local features. The second-type decision measure considers the differences of adjacent pixel values in the rank ordered median filtering sequence and the third-type approach, called switching schemes, first applies several types of rank-ordered filters, and then, detects the noisy pixels by their relationships with the gray level of the origin pixel.[14] In this paper, a fixed grid WN is proposed for noise detection. The input layer of WN consists of two nodes corresponding to the GD and ABD are assigned to each R, G, and B matrices (for color images) in the 3×3 sliding window. The second layer is the hidden layer that consists of several wavelet neurons (in our experiments nine, ten or twelve) are determined using OLS algorithm. The output layer includes one node that represents the identified attribution of the pixel: noisy or not-noisy. The two features in the input layer are discussed as follows:[14]

Gray-Level Difference

The GD represents the accumulated variations between the central pixel and its neighbor local pixels. It is defined as

$$GD=\sum_{\substack{j=-1\\(i,j)\neq(0,0)}}^{1}\sum_{j=-1}^{1}\left|P(0,0)-P(i,j)\right| \quad (11)$$

where $P(0,0)$ is the reference pixel and $P(i,j)$ is the surrounding local pixel. GD is a measure of noise in the flat area. It is expected that the corrupted pixels would yield much bigger differences as compared with the uncorrupted pixels. However, the pixels on edges and or texture areas will also get high GD values so that the obscure region identification between the noise, edge and texture pixels should be relied on the other assistant features, such as ABD.

Average Background Difference

Averaging the surrounding pixels as the background luminance of the sliding block to compare with the central pixel is another assistant feature to detect the noise. This feature, called the ABD, representing the overall average variation with the central pixel in the block, is defined as

$$ABD = \left| P(0,0) - \frac{\sum_{j=-1}^{1}\sum_{\substack{j=-1 \\ (i,j)\neq(0,0)}}^{1} |P(i,j)|}{8} \right| \quad (12)$$

The corrupted pixels will yield bigger differences as compared with the clean ones. For the pixels in the texture area, the GD value is large but the ABD feature is small. In order to train the proposed WN for noise detection, the X-ray, CT, MRI, US or Dermoscopy image with (20%) salt and pepper noise is used as a reference pattern for training. Also, 500 noisy pixels and 500 uncorrupted pixels uniformly distributed in the image are adopted as the training data. If the (i, j) pixel is the noisy pixel the desired output is 1 ($y(i, j)=1$)) and If the (i, j) pixel is the clean pixel the desired output is -1 ($y(i, j)=-1$).

Noise Cancelling Algorithm

After the first level, 3×3 median filter is applied for processing. WN recognizes the pixels of an image as noisy or clean, then if the pixel is noisy its value will be replaced by its median value and if it is not noisy its value will remain unchanged. This is realized as follows:

$$f(i,j) = \begin{cases} medianf(i,j) & if \;\; y(i,j) = 1 \\ f(i,j) & if \;\; y(i,j) = -1 \end{cases}. \quad (13)$$

The proposed two-level noise removal algorithm is very effective to suppress the impulse noise as well as to preserve the sharpness of edges and color detail information.

EXPERIMENTAL RESULT

In this section, the quantificational calculation and vision comparison are used to show the performance of the proposed impulse noise removal technique. The signal noise ratio (SNR) and peak signal noise ratio (PSNR) are.

$$SNR = 10\log\frac{\sum_{i=1}^{M}\sum_{j=1}^{N}(f(i,j)-\overline{f}(i,j))^2}{\sum_{i=1}^{M}\sum_{j=1}^{N}(f(i,j)-\hat{f}(i,j))^2} \quad (14)$$

$$PSNR = 10\log\frac{255^2}{\frac{1}{MN}\sum_{i=1}^{M}\sum_{j=1}^{N}(f(i,j)-\hat{f}(i,j))^2}, \quad (15)$$

where MN is the size of the image, f is the noisy image, $\hat{f}$ is restored the image and $\overline{f} = \frac{1}{MN}\sum_{i=1}^{M}\sum_{j=1}^{N}(f(i,j))^2$ is the mean of the corrupted image.

X-Ray Images

X-ray technology is the oldest and most commonly used form of medical imaging. X-rays use ionizing radiation to produce images of a person's internal structure by sending X-ray beams through the body, which are absorbed in different amounts depending on the density of the material. X-ray images are typically used to evaluate broken bones, cavities, swallowed objects, lungs, blood vessels and breasts (mammography).[27]

Here, for impulse noise canceling from X-ray images a fixed grid WN with three hidden layers, two inputs and one output is used. In our experiments, ten nodes in the hidden layer are enough. In Table 1, the PSNR of the proposed method is compared with that of many other well-known algorithms. The test image is neck X-ray image, which is corrupted by 20% impulse noise (noise density (ND=20%). The results show that our denoising method performs better than the other methods.

A comparison between proposed WN (with ten neurons) denoising, VMF, adaptive median filter (AMF) and NN (with 25 neurons) for neck X-ray test image is shown in Figure 2 with noisy images (NI) as an addition. Figure 3 shows the same results.

CT Images

Computed tomography (CT), also commonly referred to as a CAT scan, is a medical imaging method that combines multiple X-ray images taken from different angles to produce detailed cross-sectional pictures of areas inside the body. The resulting images provide more information than regular X-rays, and allow doctors to look at individual slices within the 3-D images. CT is often used to evaluate organs in the

Table 1: Comparison of restoration result in PSNR (dB) for ND= 20% for chest X-ray image

Algorithm	PSNR
Noisy image	25.36
Vector median filter	28.75
Adaptive median filter	31.63
Neural network	32.31
Wavelet network (proposed)	33.45

PSNR - Peak signal noise ratio; ND - Noise densities

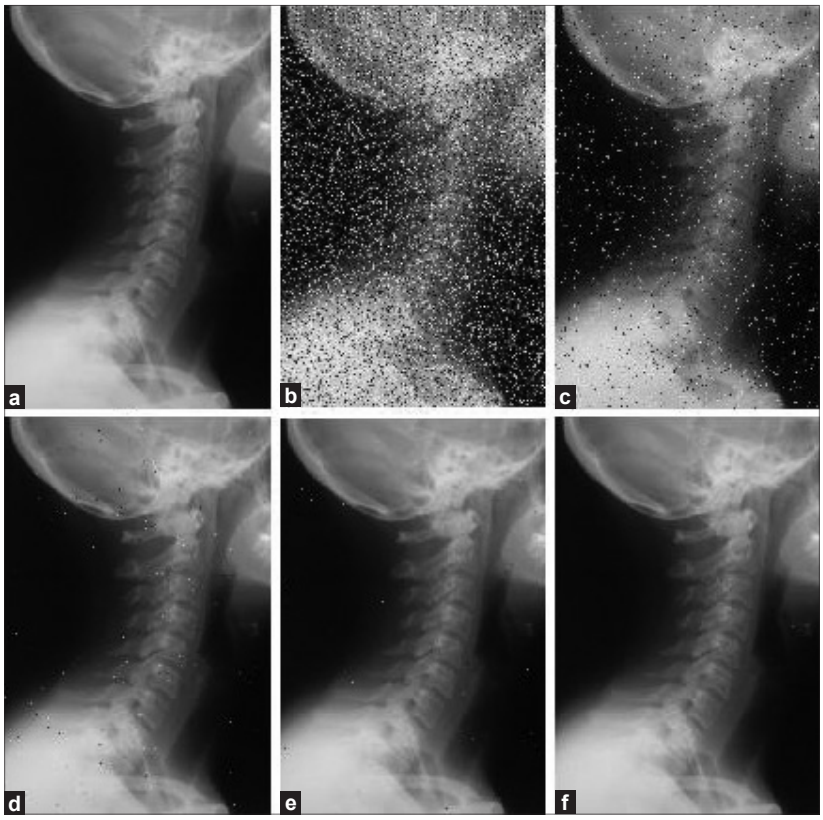

Figure 2: Contrast of filters output for neck X-ray image. (a) original image; (b) the image corrupted by impulse noise (the noise density is 20%); (c) reconstructed by vector median filtering; (d) reconstructed by adaptive median filter; (e) reconstructed by neural network (with 25 neurons); (f) reconstructed by the proposed filter.

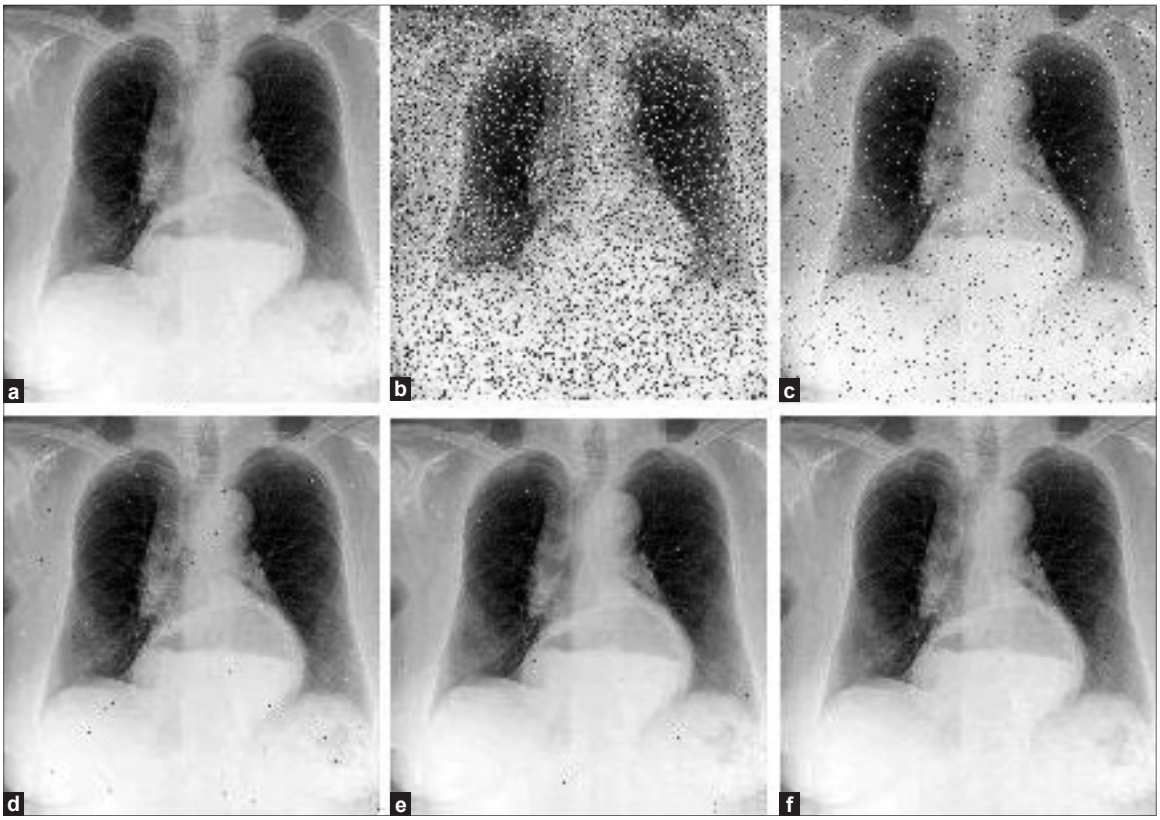

Figure 3: Contrast of filters output for chest X-ray image. () original image; (b) the image corrupted by impulse noise (the noise density is 20%); (c) reconstructed by vector median filtering; (d) reconstructed by adaptive median filter; (e) reconstructed by neural network (with 25 neurons); (f) reconstructed by the proposed filter.

pelvis, chest and abdomen, colon health (CT colonography), presence of tumors, pulmonary embolism (CT angiography), abdominal aortic aneurysms (CT angiography), and spinal injuries.[27]

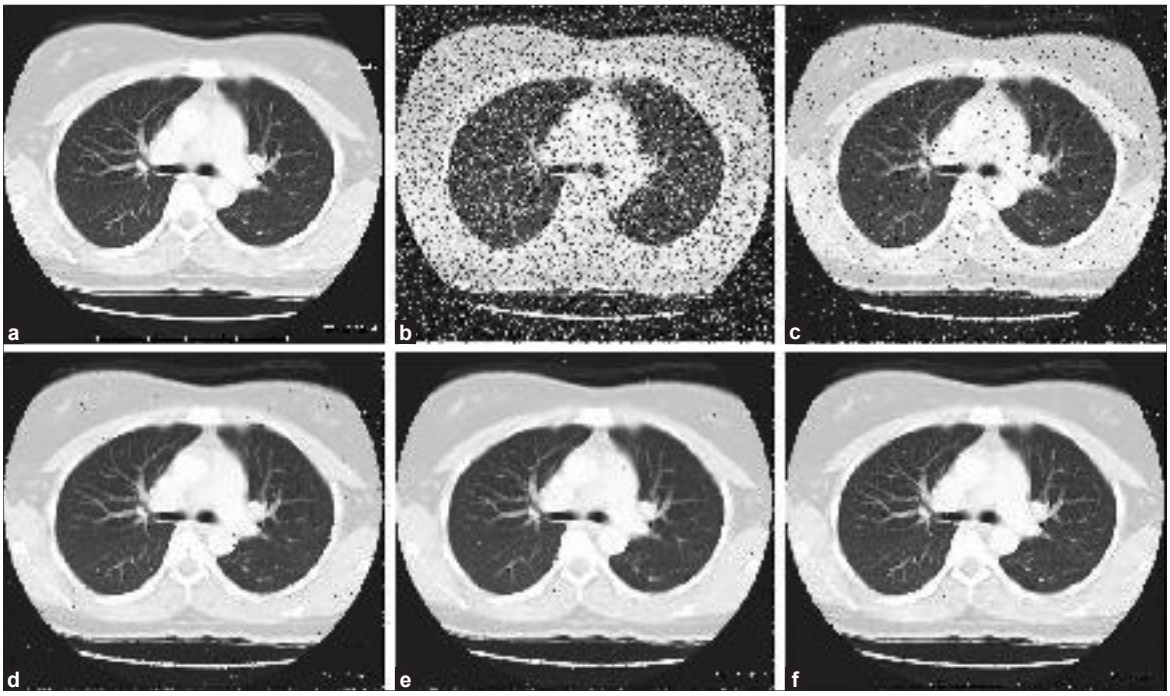

Figure 4: Contrast of filters output for lung CT image. (a) original image; (b) the image corrupted by impulse noise (the noise density is 20%); (c) reconstructed by vector median filtering; (d) reconstructed by adaptive median filter; (e) reconstructed by neural network (with 25 neurons); (f) reconstructed by the proposed filter.

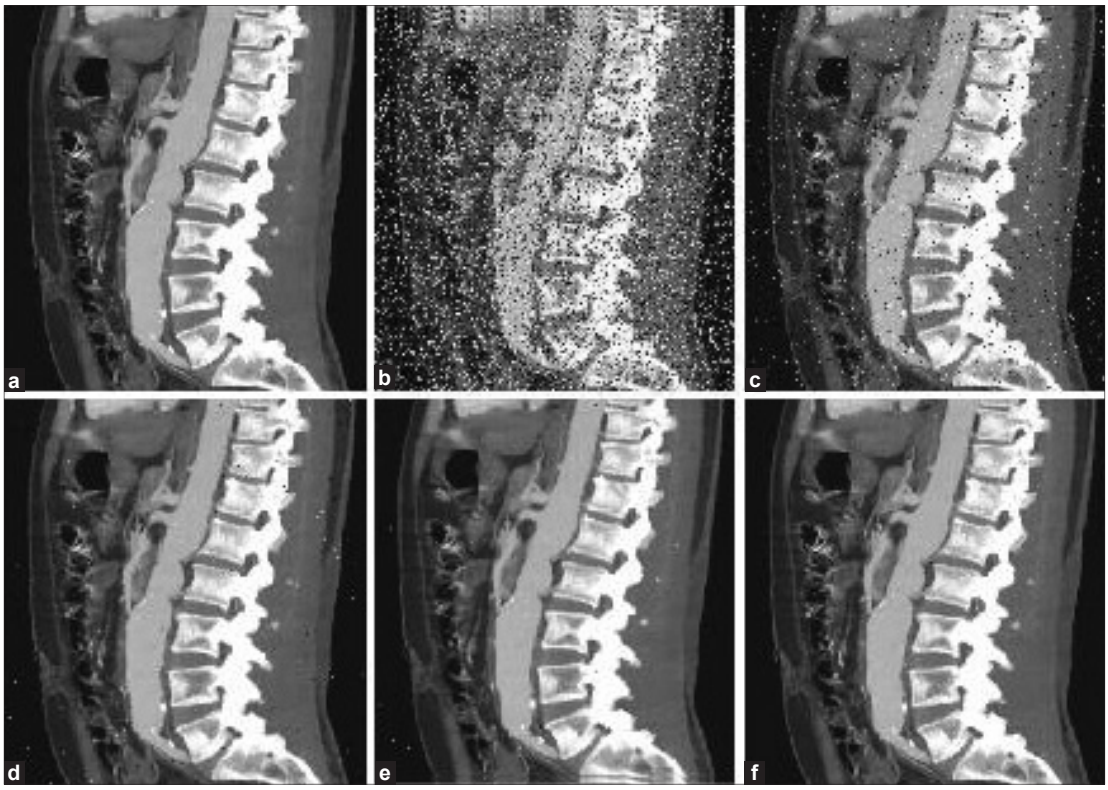

Figure 5: Contrast of filters output for loin CT image. (a) original image; (b) the image corrupted by impulse noise (the noise density is 20%); (c) reconstructed by vector median filtering; (d) reconstructed by adaptive median filter; (e) reconstructed by neural network (with 25 neurons); (f) reconstructed by the proposed filter.

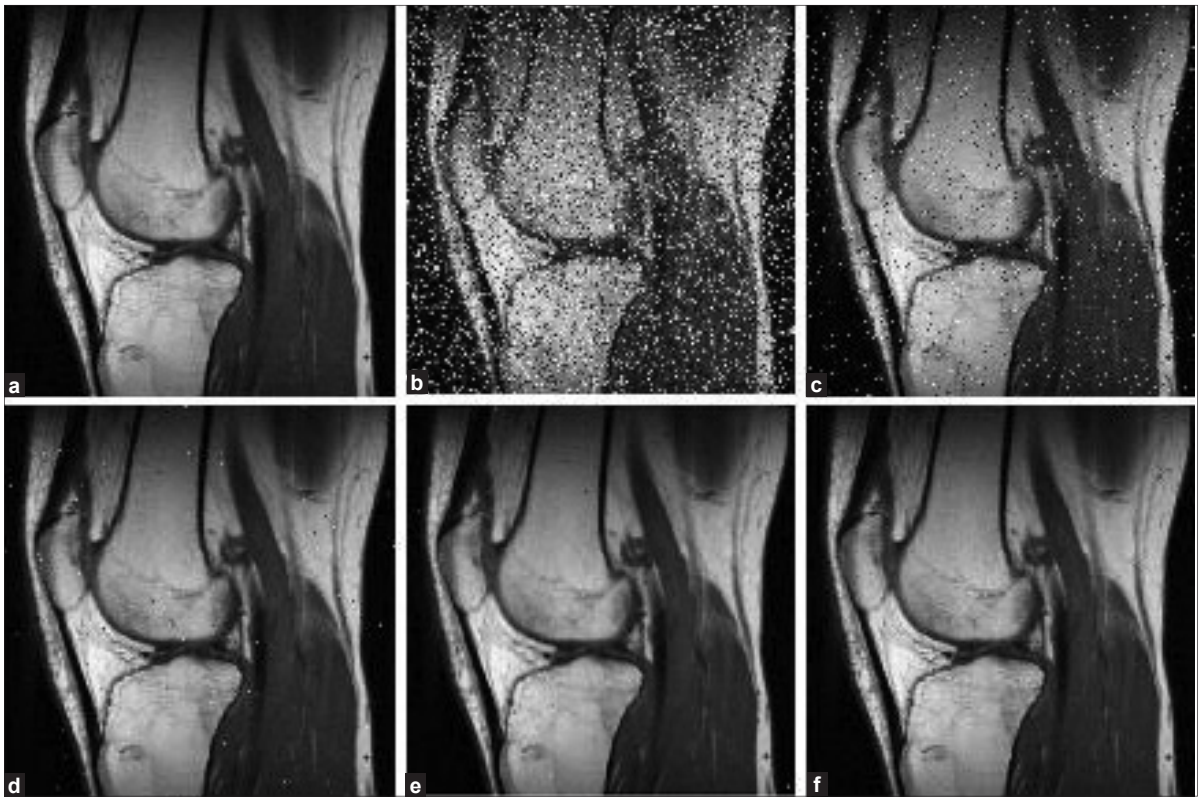

Figure 6: Contrast of filters output for knee MRI image. (a) original image; (b) the image corrupted by impulse noise (the noise density is 20%); (c) reconstructed by vector median Filtering; (d) reconstructed by adaptive median filter; (e) reconstructed by neural network (with 25 neurons); (f) reconstructed by the proposed filter.

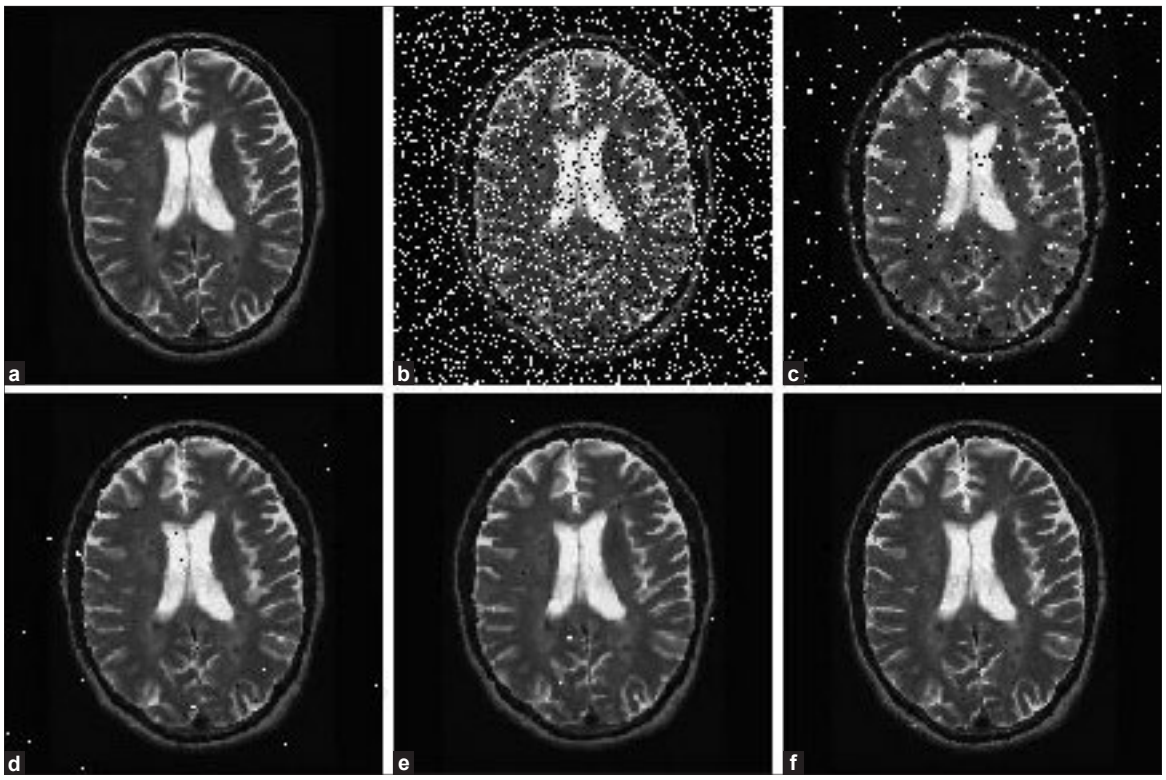

Figure 7: Contrast of filters output for brain MRI image. (a) original image; (b) the image corrupted by impulse noise (the noise density is 20%); (c) reconstructed by vector median filtering; (d) reconstructed by adaptive median filter; (e) reconstructed by neural network (with 25 neurons); (f) reconstructed by the proposed filter.

Here, for impulse noise canceling from CT images, a fixed grid WN with three hidden layers, two inputs and one output is used. In our experiments, twelve nodes in the hidden layer are enough. Table 2 gives a comparison of SNR indicates for different noise densities (ND) for lung CT image test. A comparison between proposed WN (with twelve neurons) denoising, VMF, AMF and NN (with 22 neurons) for lung and loin CT test images is shown in Figures 4 and 5 respectively.

MRI Images

Magnetic resonance imaging (MRI) is a medical imaging technology that uses radio waves and a magnetic field to create detailed images of organs and tissues. MRI has proven to be highly effective in diagnosing a number of conditions by showing the difference between normal and diseased soft tissues of the body. MRI is often used to evaluate blood vessels, breasts, organs in the pelvis, chest and abdomen (heart, liver, kidney, spleen).[28]

Here, in this study for impulse noise canceling from MRI images, a fixed grid WN with three hidden layers, two inputs and one output is used. In our experiments, nine nodes in the hidden layer are enough. A comparison between proposed WN (with nine neurons) denoising, VMF, AMF and NN (with 23 neurons) for brain and knee MRI images is shown in Figures 6 and 7 respectively.

In Figure 8, a comparison between proposed WN (with nine neurons) denoising, VMF, AMF and NN (with 23 neurons) for brain MRI test image with different noise density is shown with noisy images (NI) as an addition. The results show that our denoising method performs better than the other methods for all different noise densities.

Ultra Sound Images

Diagnostic ultrasound (US), also known as medical sonography or ultrasonography, uses high frequency sound waves to create images of the inside of the body. The ultrasound machine sends sound waves into the body and is able to convert the returning sound echoes into a picture. Ultrasound technology can also produce audible sounds of blood flow, allowing medical professionals to use both sounds and visuals to assess a patient's health. Ultrasound is often used to evaluate pregnancy, abnormalities in the heart and blood vessels, organs in the pelvis and abdomen, symptoms of pain, swelling and infection.[27]

In this paper for impulse noise canceling from US images, a fixed grid WN with three hidden layers, two inputs and one output is used. In our experiments, ten nodes in the hidden layer are enough. In Table 3, the PSNR of the proposed method is compared with other algorithms. The test image is tummy US image, which is corrupted by 20% impulse noise (ND= 20%).

A comparison between proposed WN (with ten neurons) denoising, VMF, AMF and NN (with 21 neurons) for tummy and womb US test images is shown in Figures 9 and 10 respectively.

Dermoscopy Images

Dermatoscopy (also known as dermoscopy or epiluminescence microscopy) is the examination of skin lesions with a dermatoscope. This traditionally consists of a magnifier, a nonpolarized light source, a transparent plate and a liquid medium between the instrument and the skin, and allows inspection of skin lesions unobstructed by skin surface reflections. Modern dermatoscopes dispense with the use of

Table 2: Comparison of restoration result in SNR (dB) for different impulse noise for loin CT image

ND (%)	NI	VMF	AMF	NN	WN (proposed)
10	10.27	11.23	12.55	12.95	13.25
20	8.11	9.02	9.16	10.25	11.23
45	5.43	6.65	6.71	7.07	7.89
60	4.41	5.05	5.91	6.07	6.89
70	3.91	4.95	5.88	5.90	6.69
80	3.82	4.51	4.93	5.64	6.01

SNR – Signal noise ratio; CT – Computed tomography; ND – Noise densities; NI – Noisy images; VMF – Vector median filter; AMF – Adaptive median filter; NN – Neural network; WN – Wavelet network

Table 3: Comparison of restoration result in PSNR (dB) for ND= 20% for chest tummy US image

Algorithm	PSNR
Noisy image	36.78
Vector median filter	38.05
Adaptive median filter	38.73
Neural network	39.81
Wavelet network (proposed)	40.01

PSNR – Peak signal noise ratio; ND – Noise densities

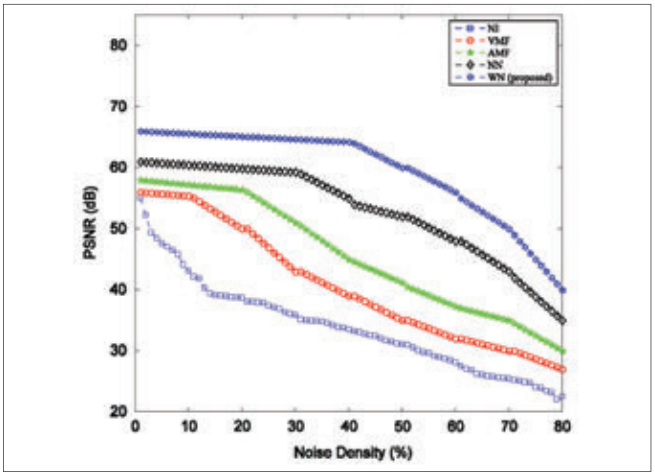

Figure 8: Denoising results (PSNR) for brain MRI image with different noise densities.

liquid medium and instead use polarized light to cancel out skin surface reflections.[29]

In this study, impulse noise canceling from Dermatoscopy images, a fixed grid WN with three hidden layers, two inputs and one output is used. In our experiments, ten nodes in the hidden layer are enough. Table 4 shows the comparison about SNR indicates for different noise densities (ND) for skin dermoscopy test images. A comparison between proposed WN (with ten neurons) denoising, VMF, AMF and NN (with 24 neurons) for dermoscopy images is shown in Figures 11 and 12 respectively.

Table 4: Comparison of restoration result in SNR (dB) for different impulse noise for LOIN CT image

ND (%)	NI	VMF	AMF	NN	WN (proposed)
10	12.27	12.43	12.55	12.95	13.25
20	11.11	11.12	11.16	11.25	12.23
45	7.43	7.65	7.71	8.07	8.89
60	6.41	7.05	7.91	8.07	8.89
70	5.91	5.95	6.88	6.90	7.69
80	4.82	5.51	5.93	6.64	7.01

SNR – Signal noise ratio; CT – Computed tomography; ND – Noise densities; NI - Noisy images; VMF – Vector median filter; AMF – Adaptive median filter; NN – Neural network; WN – Wavelet network

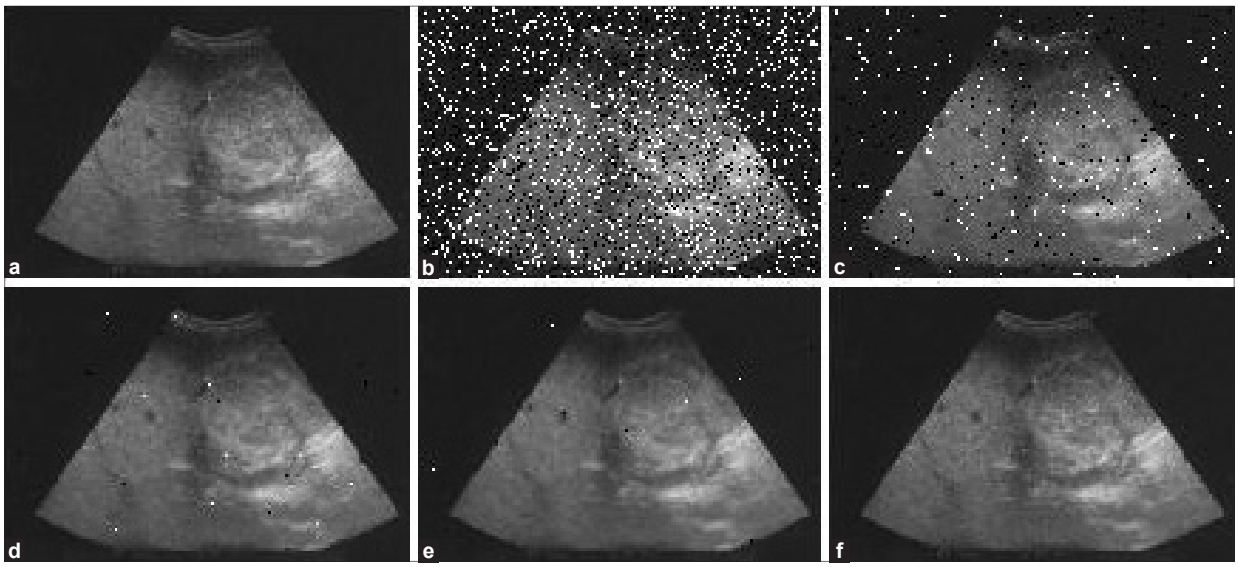

Figure 9: Contrast of filters output for tummy US image. (a) original image; (b) the image corrupted by impulse noise (the noise density is 20%); (c) reconstructed by vector median filtering; (d) reconstructed by adaptive median filter; (e) reconstructed by neural network (with 25 neurons); (f) reconstructed by the proposed filter.

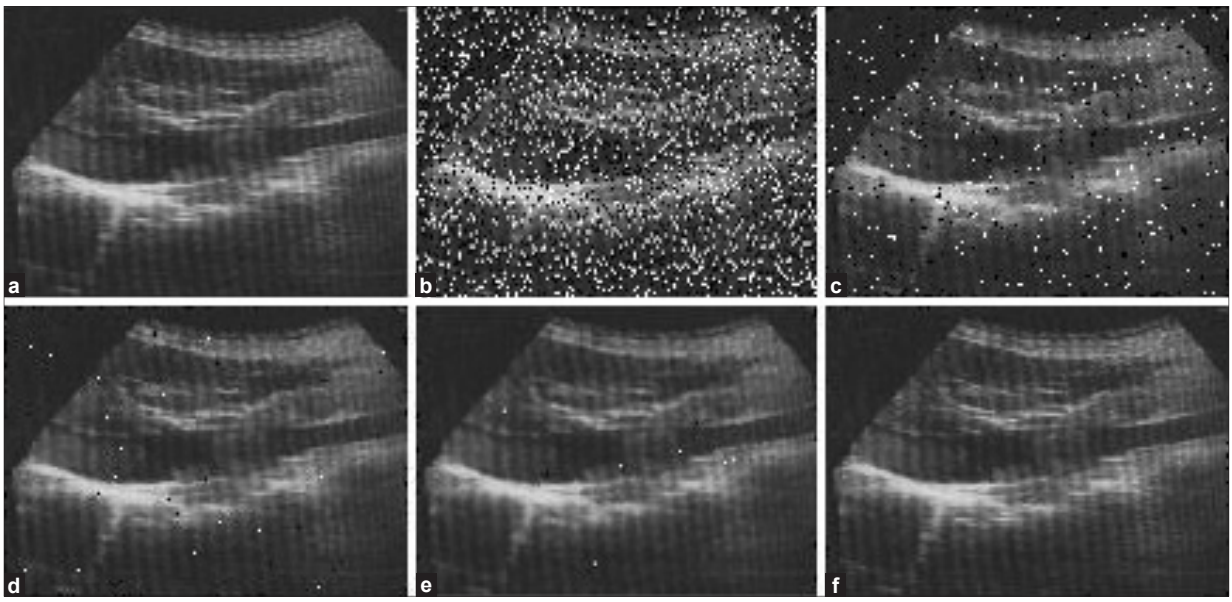

Figure 10: Contrast of filters output for wome US image. (a) original image; (b) the image corrupted by impulse noise (the noise density is 20%); (c) reconstructed by vector median filtering; (d) reconstructed by adaptive median filter; (e) reconstructed by neural network (with 25 neurons); (f) reconstructed by the proposed filter.

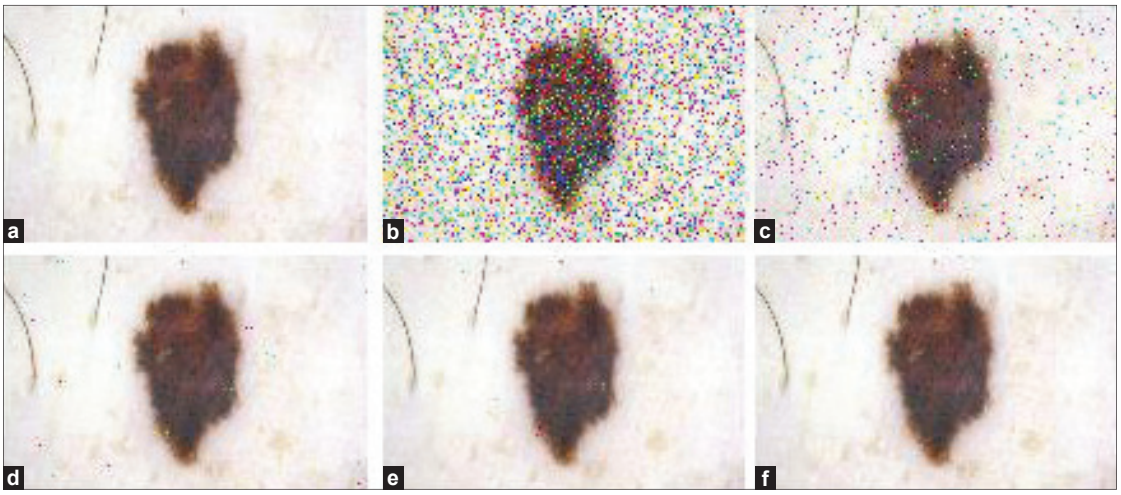

Figure 11: Contrast of filters output. (a) original image; (b) the image corrupted by impulse noise (the noise density is 20%); (c) reconstructed by vector median filtering; (d) reconstructed by adaptive median filter; (e) reconstructed by neural network (with 25 neurons); (f) reconstructed by the proposed filter.

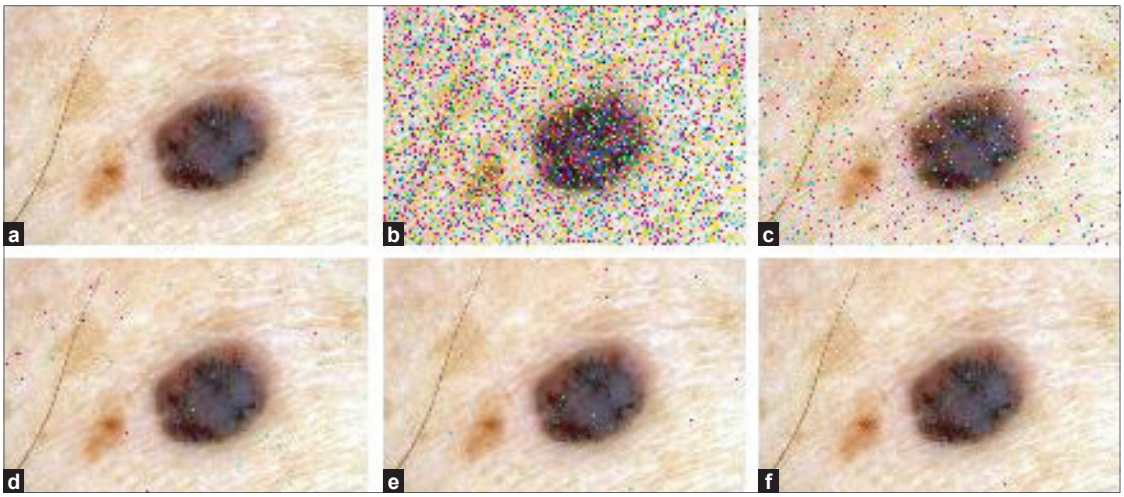

Figure 12: Contrast of filters output. (a) original image; (b) the image corrupted by impulse noise (the noise density is 20%); (c) reconstructed by vector median filtering; (d) reconstructed by adaptive median filter; (e) reconstructed by neural network (with 25 neurons); (f) reconstructed by the proposed filter.

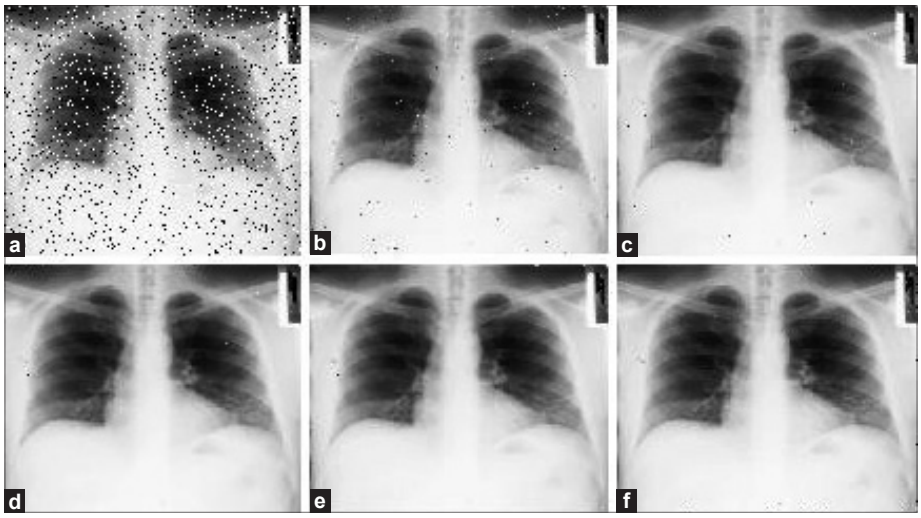

Figure 13: Contrast of filters output for real noisy chest X-ray image. (a) original image; (b) reconstructed by median Filter (c) reconstructed by vector median filtering; (d) reconstructed by adaptive median filter; (e) reconstructed by neural network (with 26 neurons); (f) reconstructed by the proposed filter (with 10 neurons).

Table 5: Comparison of restoration result in SNR and PSNR (dB) for chest X-ray image with real impulse noise

	RNI	MF	VMF	AMF	NN	WN
SNR (dB)	7.66	9.12	9.33	9.61	9.65	10.02
PSNR (dB)	10.02	12.05	12.92	13.13	13.15	13.62

Figures are in percentage; SNR – Signal noise ratio; PSNR – Peak signal noise ratio; RNI – Real noisy image; MF – Median filter; VMF – Vector median filter; AMF – Adaptive median filter; NN – Neural network; WN – Wavelet network

Real Impulse Noisy Image

Figure 13a shows an X-ray image of chest that has real impulse noise[30] (impulse noise is not added to this image; rather it naturally has the salt and paper noise). Algorithms, median filter (MF), VMF, AMF and NN (with 26 neurons) as well as own approach applied to this image. The results of this process are presented in Figure 13. As depicted, WN algorithm for image with natural noise works better than other methods.

In order to examine the details of results, parameters SNR and PSNR of this image are presented in Table 5. In this Table, the SNR and PSNR of the proposed method are compared with Real noisy image (RNI), VMF, AMF and NN. The results show that our denoising method performs better than the other methods. In addition compared to the other methods, it can efficiently preserve image details.

CONCLUSION

In this paper, a new efficient impulse noise removal based on fixed grid WN without learning is presented. The advantages of the WN, together with two powerful features GD and ABD, are combined to detect the impulse noise and then to cancel it with median filter. Extensive computer simulations with two factors (SNR and PSNR) indicate that the proposed technique can suppress impulse noise and simultaneously preserve more finer details which significantly outperforms several other algorithms such as VMF, AMF and NN.

ACKNOWLEDGMENT

This study was supported by the Medical Image and Signal Processing Research Center of Isfahan University of Medical Sciences.

REFERENCES

1. Xue-jun Z, Hong G, Yun-ting Z, Ying L, Li G. Educational practice of computer science in medical imaging. *IEEE Proceeding.* Education Technology and Computer Science. vol. 3. 2010. p. 546-9.
2. Gravel P, Beaudoin G, De Guise JA. A method for modeling noise in medical images. IEEE Trans Med Imaging 2004;23:1221-31.
3. Abreu E, Lightstone M, Mitra SK, Arakawa K. A New efficient approach for the removal of impulse noise from highly corrupted images. IEEE Trans Image Process 1996;5:1012-25.
4. Rytsar YB, Ivasenko IB. Application of (alpha, beta)-trimmed mean filtering for removal of additive noise from images. *SPIE Proceeding*. Optoelectronic and Hybrid Optical/Digital Systems for Image Processing; 1997, p. 45-52.
5. Sawant A, Zeman H, Muratone D, Samant S, DiBianca F. Adaptive median filter algorithm to remove impulse noise in x-ray and CT images and speckle in ultrasound images. *SPIE Proceeding* Medical Imaging; 1999, p. 1263-74.
6. Chunhui Z, Qingbin X, Wei N. Study on the noise attenuation characteristics of generalized morphological filters. *SPIE Proceeding* Medical Imaging; 1998, p. 236-9.
7. Runtao D, Venetsanopoulos A. Generalized homomorphic and adaptive order statistic filters for the removal of impulsive and signal dependent noise. IEEE Trans Circuits Syst 2003;34:948-55.
8. Karthikeyan K, Chandrasekar C. Speckle Noise Reduction of Medical Ultrasound Images using Bayesshrink Wavelet Threshold. Int J Comput Appl 2011;22:8-14.
9. Wang L, Lu J, Li Y, Yahagi T, Okamoto T. Noise reduction using wavelet with application to medical X-ray image. International Conference on Industrial Technology, vol. 20, 2005. p. 33-8.
10. Cheng Y, Li Y, Xue D. Image Denoising Method Based on Curvelet Cycle Spinning, *International Conference on Wireless Communications, Networking and Mobile Computing*, vol. 13, 2008. pp. 1-3.
11. Russo F, Ramponi F. A Fuzzy filter for images corrupted by impulse noise. IEEE Trans Image Process 2000;3:168-70.
12. Anisha K, Wilscy M. Impulse noise removal from medical images using fuzzy genetic algorithm. Int J Multimed Appl 2011;3:93-106.
13. Astola J, Haavisto P, Neuovo Y. Vector median filters. *IEEE Proceeding* Image Processing, vol 78. 1990, p. 678-89.
14. Liang SF, Lu SM, Chang JY, Lin CT. A Novel two-stage impulse noise removal technique based on neural networks and fuzzy decision. IEEE Trans Fuzzy Syst 2008;16:863-73.
15. Hore JE, Qiu B, Wu HR. Improved color image vector filtering using fuzzy noise detection. Opt Eng 2003;42:1656-64.
16. Pati YC, Krishnaprasd PS. Analysis and synthesis of feed-forward neural networks using discrete affine wavelet transformations. IEEE Trans Neural Netw 1993;41:73-5.
17. Zhang QH, Benveniste A. Wavelet networks. IEEE Trans Neural Netw 1992;3:889-98.
18. Zhang QH. Using wavelet network in nonparametric estimation. IEEE Trans Signal Process 1997;8:227-36.
19. Oussar Y, Dreyfus G. Initialization by selection for wavelet network training. Neurocomput 2000;34:131-43.
20. Lien C, Huang C, Chen P, Lin Y. An efficient denoising architecture for removal of impulse noise in images. IEEE Trans Comput 2012;2: 351-60.
21. Sulamiman SN, Isa N. Denoising-based clustering algorithms for segmentation of low level salt-and-pepper noise-corrupted images. IEEE Consum Electron 2011;56:2702-10.
22. Toh K, Isa N. Noise Adaptive fuzzy switching median filter for salt-and-pepper noise reduction. IEEE Trans Signal Process 2010;17:281-4.
23. Jiang X. Iterative truncated arithmetic mean filter and its properties. IEEE Trans Image Process 2012;21:1-11.
24. Galvao R, Becerra VM, Calado MF. Linear –wavelet networks. Int J Appl Math Comput Sci 2004:14:221-32.
25. Billings SA, Wei HL. A new class of wavelet networks for nonlinear system identification. IEEE Trans Neural Netw 2005;16:862-74.
26. Yilmaz S, Oysal Y. Fuzzy wavelet neural network models for prediction and identification of dynamical systems. IEEE Trans Neural Netw 2010;21:1599-609.
27. Duncan M. Engineering concepts on Ice. Available from: http://

www.spectro.com/pages/e/p0105.htm. [Last accessed on 2010 Oct 25].

28. Kwan BY, Kwan HK. Impulse noise reduction in brain magnetic resonance imaging using fuzzy filters. World Acad Sci Eng Technol 2011;60:1194-7.
29. Silveria M, Nascimento JC, Marques JS, Maral AR, Mendona T, Yamauchi S, *et al*. Comparison of segmentation methods for melanoma diagnosis in dermoscopy images,. IEEE Trans Signal Process 2009; 3:35-45.
30. Available from: http://www.cui.unige.ch/~svolos/SIP/ImageDenoising/Bernoulli/Image DenoisingBernoulli.html. [Last accessed on 2003 Jul 08].

How to cite this article:***

Source of Support: Nil, **Conflict of Interest:** None declared

BIOGRAPHIES

Amir Reza Sadri was born in Isfahan, Iran. He received the B.Sc. degree in electrical engineering from the Department of Electrical Engineering, University of Kashan, Kashan, Iran and the M.Sc. degree in electrical engineering from Isfahan University of Technology, Isfahan, Iran, in 2012. His research interests include system identification, signal-processing applications in control engineering, intelligent control and renewable energy.

Maryam Zekri received the Ph.D degree in Electrical Engineering (Control) From Isfahan University of Technology, Iran, in 2008. She is currently is an assistant professor in the Department of Electrical and Computer Engineering at Isfahan University of Technology. Her research interests are in the area of Soft Computing (Wavelet Network, Neural Network, Fuzzy Logic), Intelligent Control and Automatic Diagnosis of the Disease.

Saeid Sadri received the Ph.D. degree in electrical engineering from Isfahan University of Technology, Isfahan, Iran. Currently, he is with the Department of Electrical and Computer Engineering, Isfahan University of Technology. His research interests include signal processing, especially time-frequency signal analysis.

Niloofar Gheissari was born in Iran in 1977. She received the Engineering honours degree in Software Engineering from the Isfahan University of Technology, Iran, in 2000, and the Ph.D. degree from the Swinburne University of Technology, Melbourne, Australia, in 2004. Her Ph.D. thesis concerned model-based segmentation of visual data. Since 2005, she has worked in different research areas for National ICT Australia, Australian National University, Canberra, where she is currently a Postdoctorate Researcher. Her research interest is in different areas of computer vision, including segmentation, motion estimation, tracking, and object recognition.